

**WERE PRESOLAR GRAINS DESTROYED BY THE NEBULAR PROCESS RESPONSIBLE FOR THE VOLATILE ELEMENT FRACTIONATION?** J. Davidson<sup>1</sup>, H. Busemann<sup>1,2</sup>, C. M. O'D. Alexander<sup>2</sup>, L. R. Nittler<sup>2</sup>, P. Hoppe<sup>3</sup>, I. A. Franchi<sup>1</sup>, and M. M. Grady<sup>1</sup>. <sup>1</sup>PSSRI, The Open University, Walton Hall, Milton Keynes MK7 6AA, UK, <sup>2</sup>Department of Terrestrial Magnetism, Carnegie Institution of Washington, Washington, DC 20015, USA, <sup>3</sup>Max-Planck-Institut für Chemie Mainz, Germany. ([j.davidson@open.ac.uk](mailto:j.davidson@open.ac.uk)).

**Introduction:** Here we use results obtained with NanoSIMS raster ion imaging to determine the abundance of SiC in a number of CM and CR chondrites using acid-residues. These are the first steps of a more detailed study aiming to compare: (1) SiC abundances obtained by SIMS and by noble gas analyses, and (2) SiC grains from acid-residues with those concentrated by gentle physical separation techniques [1, 2].

Presolar grains were incorporated into all chondrite classes and survive in the most primitive members of each [3]. Primitive chondrites also contain abundant carbonaceous material (2-4 wt%), most of which is in insoluble organic matter (IOM) [4]. IOM and presolar grains are found in similar CI-like relative abundances in the most primitive chondrites [3, 5]. After parent body formation, both IOM and presolar grains experienced thermal and hydrothermal processing [6]. The effects of these processes are evident in the characteristics of what remains of the original IOM and presolar grains, including the abundances of SiC grains [5-8].

Even in the most primitive chondrites, there are significant variations in abundances of noble gases carried by presolar grains. This contradicts the idea of a well-mixed reservoir of presolar grains incorporated into all primitive chondrite classes. Huss *et al.* [7] suggested that these variations are the result of destruction of presolar grains in the nebula by heating to temperatures that may have exceeded 700°C. They also linked this heating to the volatile element fractionations in chondrites. Of the carbonaceous chondrites, the CRs have amongst the lowest matrix-normalized SiC abundances and largest volatile element fractionations [7]. However, the CRs contain the most primitive IOM of any chondrite class, and this IOM never experienced high temperatures [8-9]. Raman studies [10] suggest that the IOM experienced peak temperatures of <240°C. Such temperatures alone would not have affected the SiC grains or the noble gas concentrations in them. Either the IOM escaped the heating, implying that it is not presolar, or SiC was degassed/destroyed at low temperatures, perhaps during parent body processing [5]. Clearly, determining SiC abundances independently of noble gases is the first step to resolving this paradox. Ion imaging of SiC grains is a direct technique and the use of residues rather than thin sections greatly reduces the total area that needs to be analysed.

**Samples:** IOM separates from primitive CR chondrites EET 92042 (CR2), Al Rais (CR2) and GRO

95577 (CR1) were studied, along with Murchison (CM2) and Bells (anomalous CM2) (Table 1). The IOM was prepared using CsF-HF (1.6-1.7 g/cc and pH 5-7) [9] with the exception of Murchison which was prepared by HF-HCl, chromic and perchloric acid demineralization [11]. We will compare Murchison residues prepared with both techniques to see if they affect the SiC abundances.

**Experimental:** Ion images were obtained with the Cameca NanoSIMS instruments at the Open University, the Carnegie Institution of Washington, and the Max-Planck-Institut für Chemie, Mainz. For each meteorite, multiple fragments of residue were pressed into Au and ion imaged. Data were processed and analysed using L'IMAGE software (Nittler, unpub.). Total areas of residue imaged were determined and SiC grains were then identified by systematically applying suitable minimum threshold values to <sup>13</sup>C/<sup>12</sup>C “sigma” images (see Fig. 1) to identify anomalous areas. “Sigma” images display at each pixel the number of sigma that the pixel ratio is from a standard value. Candidate grains were only identified as SiC if detected <sup>13</sup>C/<sup>12</sup>C anomalies spatially correlated with high <sup>28</sup>Si/<sup>12</sup>C. Care was taken to be consistent when defining SiC grains for each meteorite, and between meteorites. Abundances were calculated using the following formula:

$$\text{SiC (ppm)} = Y * \nu * (r1/r2) * 10^6$$

Where;  $Y$  = mass fraction of the bulk meteorite in residues,  $\nu$  = area fraction of SiC grains,  $r1$  = density of SiC,  $r2$  = density of residue.

**Results:** The Murchison SiC abundance calculated here is comparable to that obtained by Huss *et al.* using noble gas tracer abundances in acid residues [7].

For Bells data, we compared microtomed IOM material with pressed fragments to see if microtoming preferentially ‘plucks’ the robust SiC grains, thereby lowering measured SiC abundances. Both microtomed and pressed samples gave similar abundances of 17 and 16 ppm, respectively (Table 1). These concentrations are slightly higher than for Murchison.

Data presented here show no noticeable difference between CR1 and CR2 chondrite SiC abundances (the very high abundance for Al Rais may be a statistical fluke: all 4 SiC grains in Al Rais have diameters well above the typical size range). This result indicates no significant impact of increasing aqueous alteration on SiC abundances. Hence, this cannot explain the dramatically different SiC concentrations measured di-

rectly here for the CRs, compared to those determined indirectly from noble gases for Renazzo [7].

Fig. 2a shows that Murchison grains give consistently lower  $^{12}\text{C}/^{13}\text{C}$  ratios than the CRs and anomalous CM2 Bells. However,  $^{12}\text{C}/^{13}\text{C}$  distributions are known to be similar for all chondrites and peak at  $\sim 50$ . Fig. 2b shows that different types of sample yield SiC grains in the same size range. Previous studies [12] indicate the number distribution should peak at 0.1-0.2  $\mu\text{m}$  (lower than seen here). These differences are likely due to contributions from surrounding material to the estimated C isotopic compositions of SiC grains embedded in the IOM (all but Murchison).

| Meteorite       |    | Analysed area ( $\mu\text{m}^2$ ) | # SiC     | PPM       | PPM [7] |
|-----------------|----|-----------------------------------|-----------|-----------|---------|
| <b>CR1</b>      |    |                                   |           |           |         |
| GRO 95577       | OU | 1126                              | 7         | 10        |         |
|                 | M  | 1961                              | 2         | 20        |         |
|                 | C  | 770                               | 5         | 32        |         |
| <b>Combined</b> |    | <b>3858</b>                       | <b>14</b> | <b>19</b> |         |
| <b>CR2</b>      |    |                                   |           |           |         |
| Renazzo         |    |                                   |           |           | 1.86    |
| Al Rais         | M  | 969                               | 4         | 120       |         |
| EET 92042       | OU | 2077                              | 19        | 16        |         |
|                 | M  | 1241                              | 3         | 9         |         |
| <b>Combined</b> |    | <b>3317</b>                       | <b>22</b> | <b>13</b> |         |
| <b>CM2</b>      |    |                                   |           |           |         |
| Murchison       | OU | 11761                             | 45        | 12        | 13.5    |
| Bells           |    | 3915                              | 5         | 16        |         |
| (Micro-tomed)   | M  | 2275                              | 3         | 17        |         |

Table 1. Abundance of SiC in bulk primitive chondrites studied here with NanoSIMS and by noble gas analyses [7]. IOM studied was in the form of picked fragments unless otherwise stated. OU = Open University, M = Mainz, C = Carnegie.

Potential sources of bias, which will lead to underestimates of abundances, include: (1) less isotopically anomalous grains will be less efficiently detected, (2) detection efficiencies will decrease as the sizes of the grains approach the order of the ion beam size because of dilution with the surrounding IOM, and (3) uncertainties in the estimated sizes of grains also associated with the ion beam size.

**Conclusions:** Ion imaging can be used to directly measure SiC abundances even from highly processed residues. We find much higher SiC abundances for CRs (Table 1) than previously estimated based on noble gases [7], and closer to what would be predicted for CI-like relative abundances. Our results are consistent with in situ observations for CRs [13], and suggest that the SiC was either degassed rather than destroyed, or only a minor gas-rich component was destroyed. Degassing would require much lower peak temperatures [400-450°C, 7] but these temperatures are too low to explain all but the most volatile element frac-

tions and are higher than the IOM experienced. Similar SiC abundances in CR1s and CR2s show that SiC was not progressively destroyed by increasing degrees of aqueous alteration. Thus, variations in the SiC noble gas abundances were probably established prior to accretion, or early on during parent body processing.

We intend to further refine our procedures for measuring abundances, as well as extend this study to other types of presolar grains and other primitive meteorite groups, such as the COs and CVs.

**References:** [1] Bernatowicz, T. J. et al. (2003) *GCA* 65, 4679-4691. [2] Tizard, J. M. et al. (2005) *MAPS* 40, 335-342. [3] Huss, G. R. and Lewis, R. S. (1995) *GCA* 59, 115-160. [4] Gilmour, I. (2003) *Treatise on Geochemistry* 1, 269-280. [5] Alexander, C. M. O'D. (2005) *MAPS* 40, 943-965. [6] Huss, G. R. et al. (2006) *MESS II*, 567-586. [7] Huss, G. R. et al. (2003) *GCA* 67, 4823-4848. [8] Busemann, H. et al. (2006) *Science* 312, 727-730. [9] Alexander, C. M. O'D. et al. (2007) *GCA* 71, 4380-4403. [10] Busemann, H. et al. (2007) *MAPS* 42, 1387-1416. [11] Russell, S. (1992) *Thesis*. [12] Amari, S. et al. (1994) *GCA* 58, 459-470. [13] Floss, C. & Stadermann, F. J. (2005) *LPSC XXXVI*, #1390.

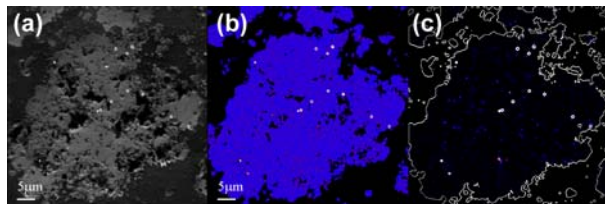


Figure 1. NanoSIMS images of Murchison residue: (a) Secondary electron image, (b)  $^{13}\text{C}/^{12}\text{C}$  map used to identify potential SiC grains on basis of  $^{13}\text{C}$  anomalies, (c)  $^{28}\text{Si}/^{12}\text{C}$  map used to verify presence of SiC grains (white circles) with residue outline.

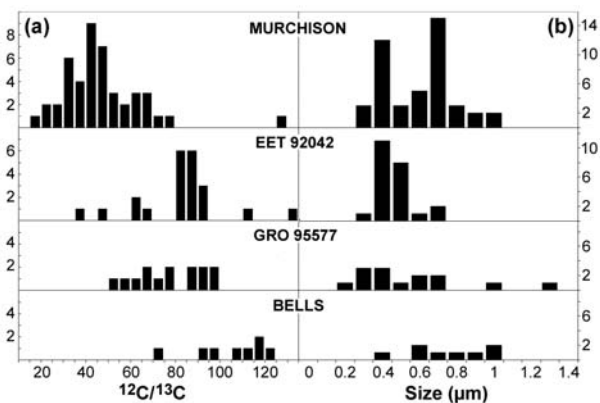


Figure 2. (a)  $^{12}\text{C}/^{13}\text{C}$  ratio for CM and CR chondrites. (b) Size distribution of SiC grains ( $\mu\text{m}$ ), Y-axes are frequency by number.